Lasers in Manufacturing Conference 2023

Influence of beam oscillation on the melt flow during laser beam fusion cutting and the resulting cut quality

Michael Sawannia[a,*], Madlen Borkmann[b], Patrick Herwig[b], Andreas Wetzig[b], Christian Hagenlocher[a], Thomas Graf[a]

[a]*Institut für Strahlwerkzeuge (IFSW), Pfaffenwaldring 43, 70569 Stuttgart, Germany*
[b]*Fraunhofer-Institut für Werkstoff- und Strahltechnik – IWS, Winterbergstr. 28, 01277 Dresden, Germany*

Abstract

Laser fusion cutting was performed of 10 mm stainless steel (AISI 304) at a power of 8 kW and a feed rate of 4.5m/min, with and without beam oscillation. To analyze the influence of the beam oscillation on the melt flow, the 3D-geometry of the cutting front was determined with a polarization goniometer at a framerate of 75000 Hz and a local resolution < 50µm. Additionally, the melt ejection was recorded with a second camera horizontal to the sample at a frame rate of 8000 Hz. During beam oscillation with a frequency of 600 Hz and an amplitude of 0.15 mm a big step is visible on the cutting front, which probably redirects the gas and hence the melt flow. The angle of the big step matches excellent to the striation pattern in the lower half of the surface of the cut edges. Additionally, the melt flow behavior inside the kerf can be estimated, considering the periodic burst like melt ejection at the bottom.

Keywords: laser beam cutting; beam oscillation; cutting front; 3D-measurement; melt flow

1. Introduction

Beam oscillation longitudinally to the feed direction provides the potential to increase the feed rate in laser cutting at a certain power level, with the oscillation frequency *f* and an amplitude *A* Goppold et al., 2020; Lind J. et al., 2021; Mahrle and Beyer, 2009. The cutting front gets flatter and longer through beam oscillation, which increases the local absorption and hence improves the efficiency Lind J. et al., 2021; Mahrle and Beyer, 2009. However, the geometry also changes periodically, which affects the melt flow out of the kerf and across

* Corresponding author. Tel.: +49(0)-711-685-66850; fax: +49(0)-711-685-66842. *E-mail address:* michael.sawannia@ifsw.uni-stuttgart.de.

the surface of the cut edge. This significantly influences the resulting cut quality in the form of striations and dross. To analyze the influence of the changing cutting front, the 3D-geometry must be determined with a high temporal (several 10 kHz) and spatial resolution (< 50 µm). This is possible with a polarization goniometer, which records the thermal emission of the cutting front and allows a subsequent 3D reconstruction of the surface geometry Sawannia et al., 2022. In this work, this technique is used and correlated with the behavior of the melt ejection, which allows conclusions about the formation of the resulting striation pattern. Furthermore, the local geometry change during one oscillation period is given for f = 600 Hz and A = 0.15 mm.

2. Experimental setup

The experimental setup is shown in Figure 1. In the study 10 mm thick stainless steel (AISI 304) was cut with an 8 kW disk laser (Trumpf, TruDisk 8001). To use 2D beam oscillation during the cutting process, the cutting head BIMO FSC from HIGHYAG was combined with a welDYNA scanner of Scanlab. A fibre with a core diameter of 100 µm was used. The focus diameter was 200 µm. The beam parameter product was 5 mm * mrad. The beam focus was set to 4.5 mm below the sample surface. The cutting gas was nitrogen with a pressure of 24 bar. A standard nozzle with an outlet diameter of 2.7 mm was used with a standoff distance of 4 mm. The sample dimensions were 100 mm x 6 mm x 10 mm (length x width x height). Cuts were performed with a length of 35 mm by moving the sample underneath the cutting head. A constant laser power of 8 kW and constant feed rate of 4.5 m/min were used for the published experiments. The beam oscillation was performed longitudinal to the feed direction (x), where the amplitude A corresponds to the maximum displacement to the arithmetic mean of a sine oscillation with the frequency f. For the following results the frequencies were varied between 50 Hz - 2000 Hz and the amplitude was set to 0.15 mm.

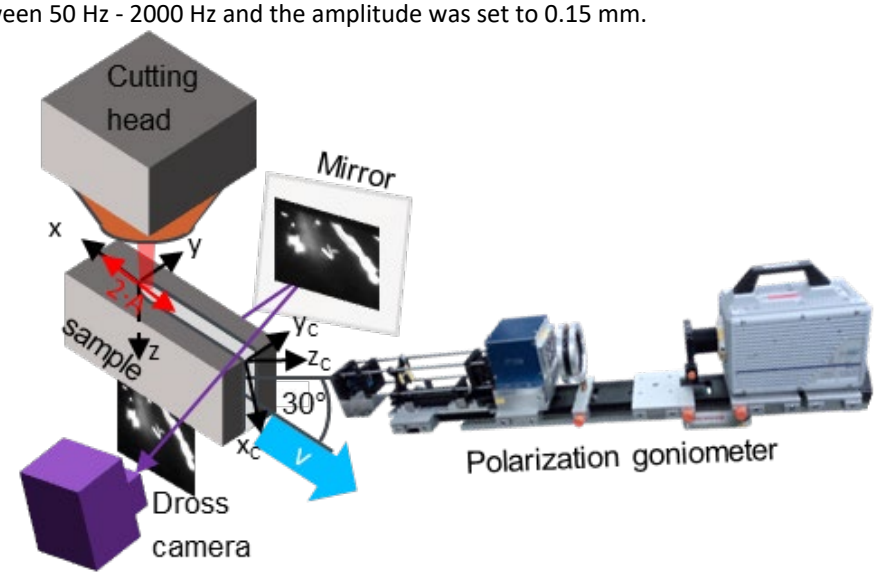

Fig. 1. Schematic sketch of the experimental setup

To determine the 3D-geometry of the cutting front, the polarization goniometer shown in Figure 1 was used to record the thermal process emission of the cutting front with a high temporal resolution of 75000 frames per second and a spatial resolution of less than 50 µm. The exposure time was 13.3 µs. Therefore, the goniometer was arranged under 30° to the sample surface in feed direction with the focus of the imaging plane

on the cutting front. It records the thermal emission after four linear polarizers with the orientations of 0°, 90°, 135° and 135°, resulting in four images on one camera frame. Two bandpass filters limit the spectrum of the measured emission. The spectral range of 850/40 nm is used for the first three single images with the different polarizer orientations. These are necessary to calculate the 3D geometry of the cutting front for each camera frame by using the polarization information, see to Sawannia et al., 2022. With the fourth image (135° polarizer orientation and the spectral range of 751/42 nm) the temperature can be determined with quotient pyrometry with the third image of the wavelength of 850 nm, which is however beyond the scope of this paper.

An additional camera was placed perpendicular to the feed rate in order to capture the melt ejection and dross at the bottom of the sample. This camera is hereinafter referred to as *dross camera*. The recording framerate of this camera was 8000 Hz and the exposure time was 86 µs. The laser was blocked with a shortpass filter $\lambda_{trans} < 950$ nm. The imaging plane was aligned almost horizontally to the sample side with a slight top view via the mirror, which additionally allowed to record the current laser beam position during beam oscillation.

3. Results

The best static cut was used as basis to investigate the influence of beam oscillation on the melt flow and the resulting cut quality, with the cut parameters mentioned above. Fig. 2 compares the results for cutting with different frequencies. The respective surface of the cut edge is shown in Fig. 2. (a), feed direction is in positive (*x*). The cut has regular striations, with the striations going down vertically in the upper quarter and then tilting slightly to the left in the bottom part. Rare and sporadic dross is visible at the bottom edge.

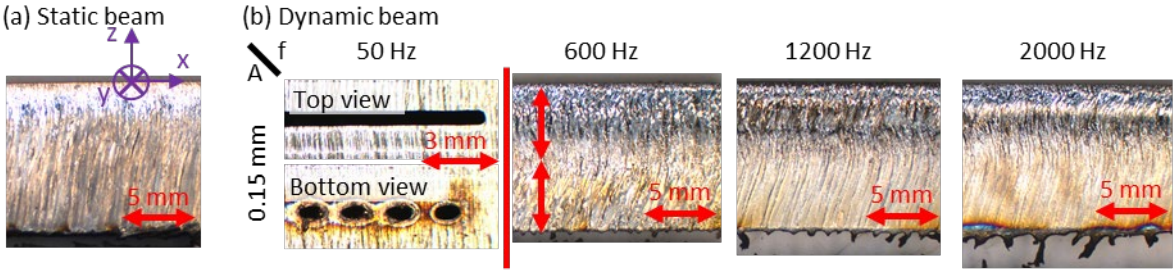

Fig. 1. Resulting surface of the cut edge for a static beam (a) with t = 10 mm, P = 8 kW, v = 4.5 m/min and dynamic beam (b) with different frequencies and an amplitude of 0.15 mm. For f = 50 Hz no separation cut was achieved, instead of the surface of the cut edge the top and bottom view are shown.

For f = 50 Hz no separating cut was achieved, instead piercing occurs at the bottom edge. The best resulting cut quality was achieved for f = 600 Hz and A = 0.15 mm, see Fig. 2 (b). The cut edge has the least amount of dross. The striation pattern starts with combination of vertical striations and an inclined pattern which can be seen more clearly at 2000 Hz. In the lower half the striations have a higher inclination against the feed direction compared to the cut with a static beam. This applies to all the cuts with $f \geq 600$ Hz. With higher frequencies the dross formation increases and inclined striation pattern at the top becomes more distinct.

A 3D-reconstruction of the cutting front for the static beam is shown in Fig 3 with its respective melt ejection. The outline of the caustics of the laser beam is given be the red lines. As indicated the whole front is irradiated by the laser. In the dross camera image, a continuous vapor plume is visible. During the video the direction of ejection alternates. The position of the melt ejection is shifted against feed direction to the vapor plume. Occasionally, a second melt ejection is visible with an even further distance from the cutting front. For

the dynamic beam one recognizes a different behavior, as depicted in Figure 3 b. The violet dashed line marks the axis around which the beam is oscillated. During dynamic beam oscillation only the part of the cutting front which is directly illuminated by the laser beam can be reconstructed for each recorded image. At the reversal points against feed direction only the bottom part can be reconstructed. For the missing parts the signal/thermal emission on the cutting front is too low. Sawannia et al., 2022 shows that the cutting front resolidifies at the positions without laser irradiation. The melt ejection at the bottom also changes, which is described in the following with the respective cutting front geometry.

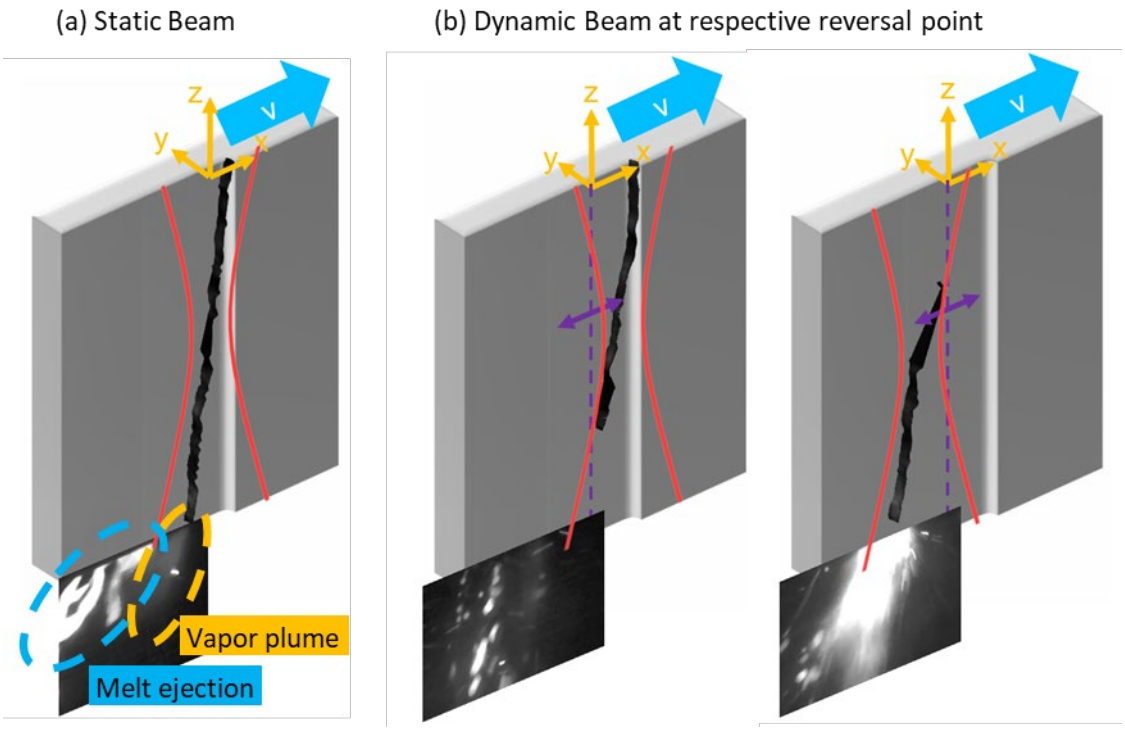

Fig. 3. 3D-reconstruction of the local cutting front with the respective melt ejection at the bottom. (a) for a static beam, (b) for a dynamic beam at the respective reversal points for longitudinal beam oscillation in feed direction.

The melt ejection was analyzed with the dross camera. The determined geometries of cutting fronts during one period T of beam oscillation are shown in Fig. for eight time steps, in case of oscillating the beam with a frequency of f = 600 Hz and an Amplitude of A = 0.15 mm. The period starts at the maximum displacement in the feed direction (x). The violet dashed line marks the axis around which the beam is oscillated. The view of the top allows to follow the laser beam position, which can be derived from the bright spots. The view of the bottom shows representative images of the melt ejection regarding the presence of melt, spatters and vapor plume. The bottom edge is not directly visible, which means, that the melt ejection could be already detached from the sample. The height of the sample is substituted by a gray bar. Marked by the orange rectangle, the respective cutting front geometry is shown, as determined from the Goniometer measurements.

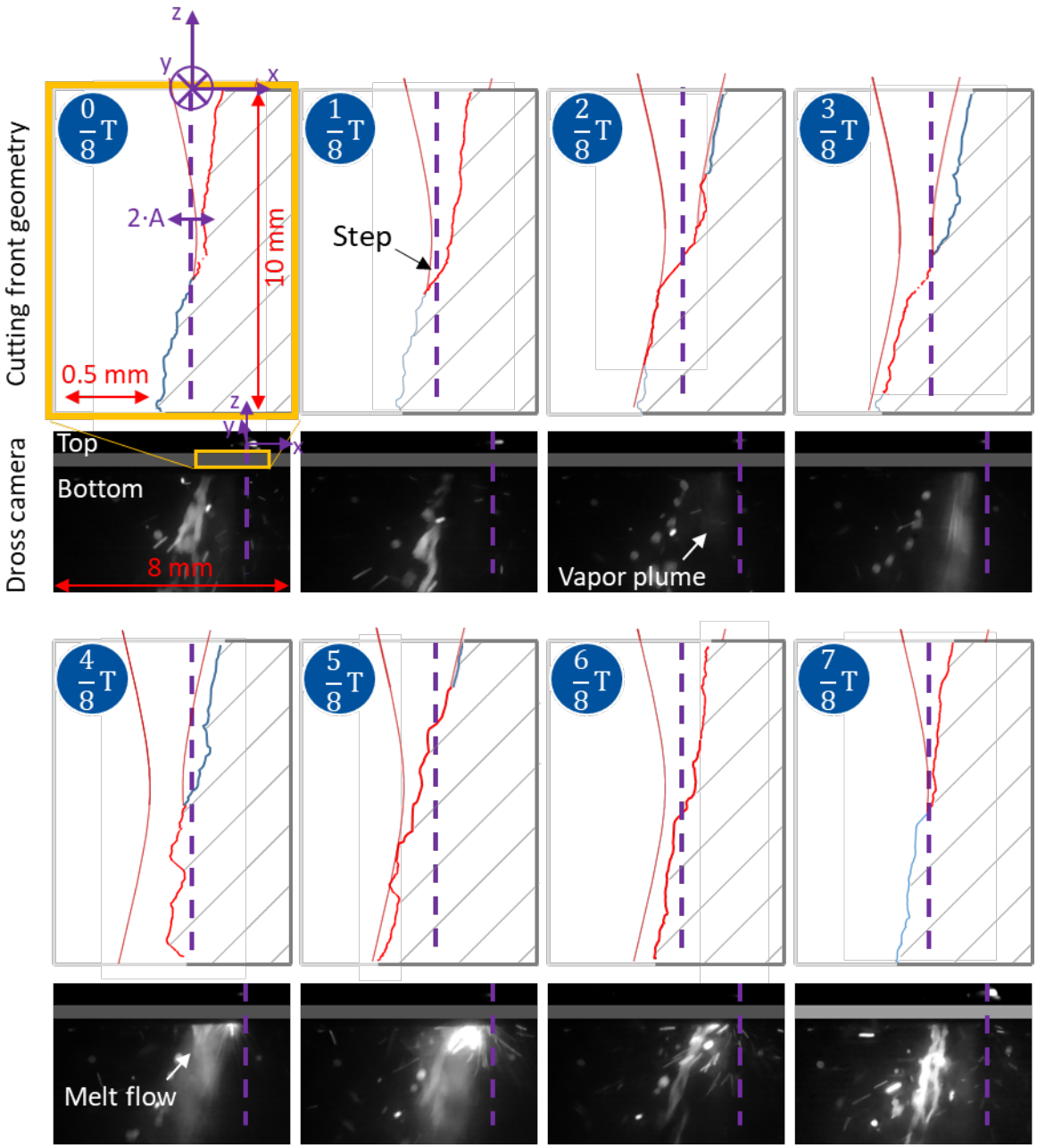

Fig. 4. One oscillation period in eight time steps. For each individual time step the determined cutting front geometry and an image of the dross camera is given. The violet dashed line marks the axis around which the beam is oscillated. The red part of the cutting front is hot/liquid, whereas the blue part is cold/solid. Additionally, the beam caustic and its current location is displayed. f = 600 Hz, A = 0.15 mm

In Fig 4 the irradiated/hot part of the cutting front is marked red, which offer a sufficient signal for the reconstruction. The cooler solid part is marked blue, which was extracted from the most recent cutting front with sufficient thermal emission. The front geometry was extracted in the *xz*-plane. The current reconstruction method builds the geometry from the top to the bottom of the sheet. Dark spots in the goniometer images and small errors in the surface angle determination result in global deviations of the total cut front shape despite the locally determined geometries are of high accuracy. As a result, the geometries are slightly too short in depth z. In order to account for this the front geometry was adapted to the sheet thickness of 10 mm by stretching the geometries in z with a factor of 1.05. The local laser position is marked by the caustic, which moves for one period around the purple dashed line with the amplitude *A*. The position of the caustic and the irradiated part of the cutting front agree remarkably well.

In the following the oscillation for one period is described. At the beginning of an oscillation period at $t = 0/8 \cdot T$ only the upper part of the cutting front is irradiated by the laser. For this segment of the period a melt flow is visible in the irradiated part, which does not move over along the solid/blue part of the cutting front. The melt ejection at the bottom could be already detached from the sample, latest at $t = 1/8 \cdot T$. Also, a big step/structure around the focus position in the middle of the sheet is visible, which is present during about 6/8 of the whole period (from $t = 6/8\ T$ to $t = 3/8\ T$). The angle of the big step agrees well with the angle of the resulting striation pattern in the lower half of the surface of the cut edge. This could indicate a detachment of the melt flow of the front and a resulting melt flow along the surface of the cut edge. The step is marked in $t = 1/8 \cdot T$, at which nearly no vapor plume is visible. In the next time step at $t = 2/8 \cdot T$, the vapor plume reappears and the cutting front starts to resolidify at the top. At $3/8 \cdot T$ the vapor plume increases together with the appearance fast spatters. At $t = 4/8 \cdot T$, only the bottom of the cutting front is irradiated and melt is excessively ejected. Most likely due to overheating and vaporization, because the laser remains longer on the same spot in the reversal point of the oscillation. Also, small spatters are visible, which are ejected in every direction, which supports the assumption of overheating. At $t = 5/8 \cdot T$ a continuous melt stream is visible with a higher distance to the beam axis (compared excessive melt ejection), which indicates a melt flow over the surface of the cut edge. At $t = 6/8 \cdot T$ a new big step is formed. The position of the ejected melt stream at the bottom moves against feed direction. At $t = 7/8\ T$ two melt streams are visible, which proves that the melt flows along the surface of the cut edges. A separated vapor plume compared to the melt flow position is visible. After this the oscillation cycle repeats.

For the higher oscillation frequencies of 1200 Hz and 2000 Hz a continuous vapor jet is visible in the records of the dross camera, which reduces significantly between $6/8 \cdot T - 1/8 \cdot T$. The melt is ejected in a similar behavior as for $f = 600$ Hz, but the melt ejection has a lower detachment angle to the work piece, which could be a reason for the higher dross formation.

4. Summary

Beam oscillation during laser cutting has a huge influence on the resulting cutting front geometry and hence the resulting cut quality. In this study the melt flow was analyzed by recording the melt ejection from the sample side and capturing the melt flow on the cutting front with a goniometer, which allowed the 3D-geometry reconstruction of the front with high temporal and spatial resolution. One oscillation period is described in detail for the frequency of 600 Hz and an amplitude of 0.15 mm. A big step is present for around 6/8 of the oscillation period in the middle of the cutting front. The position and angle of the inclined striation pattern on the surface of the cut edge in the lower half of the cutting front match with the angle and position of the step. This leads to the assumption, that the step redirects the gas flow and hence the melt flow, which creates the inclined striation pattern. The dross formation increases for oscillation frequencies above 600 Hz.

The exact reason for the enhanced dross formation in case of higher oscillation frequencies is still unclear and subject of further research.

Acknowledgements

The presented work was funded by the Deutsche Forschungsgemeinschaft (DFG, German Research Foundation) – 426328417 and Fraunhofer Gesellschaft – “FastShape”.

The Laser beam source TruDisk8001 (DFG object number: 625617) was funded by the Deutsche Forschungsgemeinschaft (DFG, German Research Foundation) – INST 41/990-1 FUGG

References

Goppold, C., Pinder, T., Schulze, S., Herwig, P., Lasagni, A., F., 2020. Improvement of Laser Beam Fusion Cutting of Mild and Stainless Steel Due to Longitudinal, Linear Beam Oscillation. Applied Sciences 10, p 3052. doi: 10.3390/app10093052

Lind, J., Wagner, J., Weckenmann, N., Weber, R., Graf, T., 2021. Investigation of the influence of beam oscillation on the laserbeam cutting process using high-speed X-ray imaging. Lasers Manuf. Conference

Mahrle, A., Beyer, E., 2009. Theoretical aspects of fibre laser cutting. J. Phys. D: Appl. Phys. 42, p 175507. doi: 10.1088/0022-3727/42/17/175507

Sawannia, M., Borkmann, M., Herwig, P., Wetzig, A., Weber, R., Graf, T., 2022. Influence of laser beam oscillation on the cutting front geometry investigated by high-speed 3D-measurements. Procedia CIRP 111, pp 736–739. doi: 10.1016/j.procir.2022.08.100